Systematic Tuning of Magnetic Properties in Mixed-Metal MOF-74

Megumi Mukoyoshi[†], Mitsuhiko Maesato[†*], Shogo Kawaguchi[‡], Yoshiki Kubota[§], Keigo Cho[‖], Yasutaka Kitagawa[‖] and Hiroshi Kitagawa[†*]*

†Division of Chemistry, Graduate School of Science, Kyoto University, Kyoto 606-8502, Japan

‡Research & Utilization Division, Japan Synchrotron Radiation Research Institute (JASRI), SPring-8,Hyogo 679-5198, Japan

§Department of Physics, Graduate School of Science, Osaka Metropolitan University, Sakai, Osaka 599-8531, Japan

‖Division of Chemical Engineering, Department of Materials Engineering Science, Graduate School of Engineering Science, Osaka University, Toyonaka, Osaka 560-8531, Japan

ABSTRACT: Recently, mixed-metal metal–organic frameworks (mixed-metal MOFs) have been attracting much attention in various fields. In this study, we have systematically investigated the magnetic properties of Co_xNi_{1-x}-MOF-74 ($Co_{2x}Ni_{2(1-x)}$(dhtp), H_4dhtp = 2,5-dihydroxyterephthalic acid) with two different kinds of metals (Co and Ni) across the composition ranges ($0 \leq x \leq 1$). Bimetallic Co_xNi_{1-x}-MOF-74 ($x = 0.752, 0.458, 0.233$) was successfully synthesized and confirmed

to have homogeneous metal distributions. Weak ferromagnetic (canted antiferromagnetic) behavior was exhibited, while homometallic Co-MOF-74 and Ni-MOF-74 are antiferromagnetic. We also investigated the effects of C_2H_4 sorption on magnetic properties and found that C_2H_4 adsorbed $Co_{0.5}Ni_{0.5}$-MOF-74 exhibited change in interchain magnetic interaction.

Metal–organic frameworks (MOFs)[1–3] are crystalline structures composed of organic ligands and metal ions, and have attracted significant interest due to their versatile nature. They are highly designable because a large number of metal elements can be used as nodes to construct MOF structures, in addition to the wide choice of organic ligands. Taking advantage of this quality, mixed-metal MOFs,[4,5] that is, MOFs that contain at least two different metal ions as nodes of their frameworks, have been recently developed in the fields of heterogeneous catalysis,[6] gas sorption,[7] gas separation,[8] luminescence,[9] and sensing.[10] By incorporating different metal ions in the same framework, it is possible to enhance stability and tune the properties of the MOF.[11] Furthermore, we can expect synergistic effects that could not be predicted from the addition of each constituent.

In this work, we report on the magnetic properties of mixed-metal MOFs with variable metal ratios to explore the relationship between the central metal ions and magnetic properties. Although magnetic properties of mixed-metal MOFs are revealed to change gradually according to their metal compositions,[12,13] there are few reports that they show different new properties from those of the parent MOFs. We focused on MOF-74, M_2(dhtp) (M = Co and Ni, H_4dhtp = 2,5-dihydroxyterephthalic acid). MOF-74 has a large cylindrical one-dimensional pore (diameter, 11 Å)[14] and consists of threefold helix chains parallel to the *c* axis (Figure 1a and 1b).[15]

Homometallic Ni-MOF-74 and Co-MOF-74 show antiferromagnetic interactions between neighboring chains at lower temperatures[15,16] with ferromagnetic (Ni) or antiferromagnetic (Co) intrachain interaction.[17] In addition, desolvated MOF-74 frameworks have open metal sites, resulting in host–guest interactions.[18] Therefore, we selected to use MOF-74 to investigate the effects of metal mixing on magnetic properties. We synthesized a series of mixed-metal Co_xNi_{1-x}-MOF-74 and investigated their magnetic properties across the composition ranges ($0 \leq x \leq 1$), confirmed that they show different magnetic properties from monometallic MOF-74. We also investigated the effects of guest sorption on magnetic properties.

Co-MOF-74 and Ni-MOF-74 were synthesized using the solvothermal methods reported previously (see the Supporting Information).[19] A series of mixed-metal Co_xNi_{1-x}-MOF-74 were synthesized by using reported method,[20] which is the same procedures as for Ni-MOF-74 and Co-MOF-74, with different ratios of metal salts: $Co(NO_3)_2$ and $Ni(NO_3)_2$. The synthesized materials were obtained as hydrates (see the Supporting Information) and as-synthesized samples were used in following measurements. The metal compositions of the synthesized materials were confirmed by XRF measurements (Table S1). The XRF results for the Co:Ni ratio were 75.2:24.8 ($Co_{0.8}Ni_{0.2}$-MOF-74), 45.8:54.2 ($Co_{0.5}Ni_{0.5}$-MOF-74), and 23.3:76.7 ($Co_{0.2}Ni_{0.8}$-MOF-74), respectively. The thermal stability was also investigated by using thermogravimetric analysis (Figure S1). As we reported previously,[21] the decomposition of Co-MOF-74 occurred higher temperature than Ni-MOF-74, and mixed-metal Co_xNi_{1-x}-MOF-74 exhibited decomposition temperatures between that of Co-MOF-74 and Ni-MOF-74, depending on their compositions.

Figure 1c shows the PXRD patterns of Co-MOF-74, Ni-MOF-74, and Co_xNi_{1-x}-MOF-74. All samples showed the typical patterns of MOF-74,[14] indicating that they are isostructural. The diffraction peaks of Co_xNi_{1-x}-MOF-74 shifted continuously to the lower angle side with increasing Co ratio (Figure 1d). This means the expansion of the lattice constant, which is consistent with the replacement of the Ni(II) ion with the larger Co(II) ion. To determine the lattice constant of the bimetallic Co_xNi_{1-x}-MOF-74, we performed the Rietveld refinement (Figures S2–6 and Tables S2–6). As shown in Figure S7, the lattice constant *a* of Co_xNi_{1-x}-MOF-74 increased, corresponding to Co content (*x*). These results support the formation of Co_xNi_{1-x}-MOF-74 where Co and Ni ions are distributed randomly and uniformly in the crystal over the whole composition range.

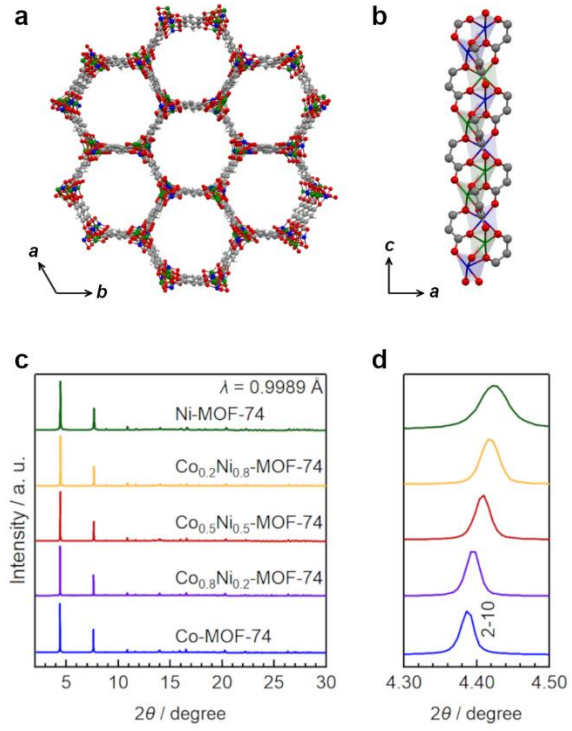

Figure 1. (a)(b) Structure of MOF-74; blue, green, red and gray spheres represent Co, Ni, O and C atoms, respectively. (c) Synchrotron PXRD patterns of Co_xNi_{1-x}-MOF-74. The radiation wavelength was 0.999 Å. (d) Close-up of the 2θ = 4.3 °–4.5 ° region.

To confirm the metal distribution, SEM observation and energy-dispersive X-ray spectroscopy (EDX) analysis were performed. Figure 2a–d shows a SEM image of $Co_{0.5}Ni_{0.5}$-MOF-74 and the corresponding Co and Ni elemental maps. The EDX maps showed that the sample has a homogeneous distribution of metals. Furthermore, EDX area analysis was performed on three regions (Figure 2e). The average Co:Ni ratio in $Co_{0.5}Ni_{0.5}$-MOF-74 was calculated to be 47.9:52.1, with a small statistic deviation (± 0.94). This result also indicates homogeneous distribution of metals for different crystals. Figures S8 and S9 show that the synthesized $Co_{0.2}Ni_{0.8}$-MOF-74 and $Co_{0.8}Ni_{0.2}$-MOF-74 also have homogeneous metal distributions.

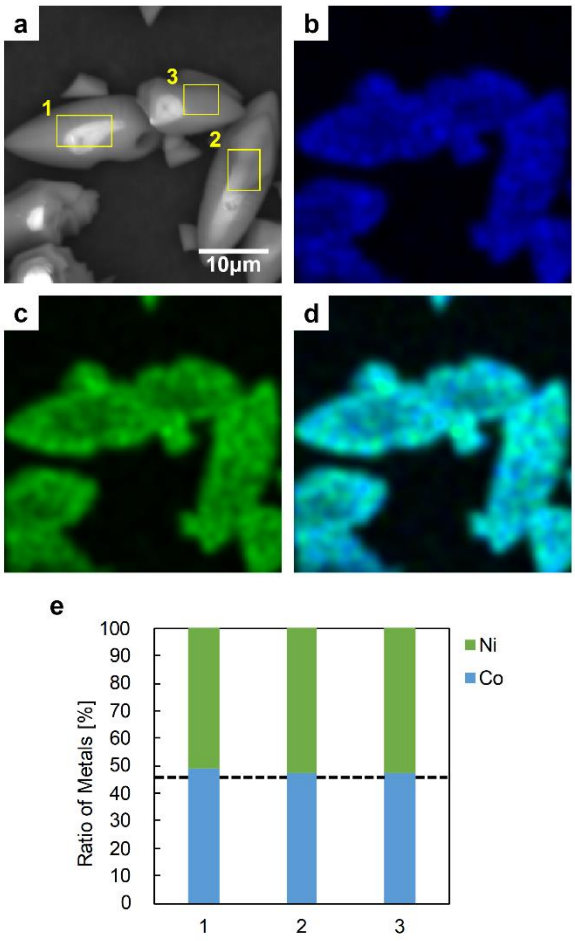

Figure 2. (a) SEM image, (b) Co-K SEM-EDX map and (c) Ni-K SEM-EDX map of $Co_{0.5}Ni_{0.5}$-MOF-74. (d) Reconstructed overlay image of the maps shown in (b) and (c). (e) Ratio of metals found in three distinct regions of $Co_{0.5}Ni_{0.5}$-MOF-74. The region where EDX data were collected to quantify the ratio of metal is shown in (a). The dashed lines in the graph show the results of XRF measurements.

In addition, the porosity of the synthesized materials was evaluated by N_2 adsorption/desorption measurements at 77 K. All the synthesized Co_xNi_{1-x}-MOF-74 showed

similar type I isotherms as Ni-MOF-74 and Co-MOF-74, indicating that they have the same porosity as homometallic MOF-74 (Figure S10). The calculated Brunauer–Emmett–Teller (BET) surface areas for $Co_{0.8}Ni_{0.2}$-MOF-74, $Co_{0.5}Ni_{0.5}$-MOF-74, and $Co_{0.2}Ni_{0.8}$-MOF-74 were 1212.3, 1191.5, and 1187.8 m^2/g, respectively. These values are almost the same as the surface areas for Ni-MOF-74 and Co-MOF-74 (Table S7).

The magnetic susceptibility of Ni-MOF-74, Co-MOF-74, and bimetallic Co_xNi_{1-x}-MOF-74 was measured (Figure 3a). Co-MOF-74 and Ni-MOF-74 exhibited antiferromagnetic transition at 7.5 K and 14.5 K, respectively. Such behavior is similar to behavior reported previously.[15,16] As the temperature decreases, the χT value of Ni-MOF-74 increases gradually and reaches the maximum value at 22.5 K and then decreases abruptly below 22.5 K (Figure S13). This behavior is due to ferromagnetic coupling of Ni^{2+} ions ($S = 1$) along the chains running parallel to the c axis and weak antiferromagnetic coupling between chains.[16] However, the χT value of Co-MOF-74 decreases gradually as the temperature decreases, showing no maximum value. This result indicates that the nature of the intrachain coupling of Co-MOF-74 is antiferromagnetic. To understand the magnetic interaction among Ni or Co ions, we performed DFT calculations using a model structure (Figure S17a) for all parallel (ferromagnetic) and anti-parallel (antiferromagnetic) spin states. First, calculated electronic structures were confirmed by spin densities on Ni ions (summarized in Table S11). Subsequently, the natural orbital analysis,[22] which is a diagonalization of the first density matrix, was performed (see the Supporting Information). As summarized in Table S12, the calculated occupation numbers of the Co model complex are smaller than the calculated values of the Ni model complex, suggesting less magnetic interaction among the Co ions in comparison with the Ni complex. These calculation

results are consistent with the temperature dependence of the magnetic susceptibility of Ni-MOF-74 and Co-MOF-74, that is, Co-MOF-74 shows antiferromagnetic transition at lower temperature than Ni-MOF-74.

In contrast to homometallic Co-MOF-74 and Ni-MOF-74, bimetallic Co_xNi_{1-x}-MOF-74 exhibited different behavior, showing weak spontaneous magnetization at 9.3 K (x = 0.752), 10.7 K (x = 0.458), and 12.5 K (x = 0.233), respectively (Figure 3b). The behavior is characteristic of weak ferromagnetism (canted antiferromagnetism). This phenomenon may be due to the Dzyaloshinskii–Moriya interaction[23,24] between different kinds of metal ions. From the ratio of the magnetization at 2 K measured on field cooling at 10 Oe (Figure S11) and an expected saturation magnetization for each material, the spin canting angle was calculated. These calculated angles were as follows: $Co_{0.8}Ni_{0.2}$-MOF-74, 0.53°; $Co_{0.5}Ni_{0.5}$-MOF-74, 0.46°; and $Co_{0.2}Ni_{0.8}$-MOF-74, 0.25°. Although similar behavior has been reported for Fe-doped Ni-MOF-74,[25] a wide range of doping was not achieved due to the unstable nature of Fe(II) ions in air. In this work, we systematically investigated the magnetic properties of mixed-metal MOF-74 across the composition ranges ($0 \leq x \leq 1$). In addition, in Fe doped Ni-MOF-74 system, Rubio *et al.* showed that lower Fe doping provides larger spontaneous magnetization because intrachain spin canceling occurs with higher Fe doping. However, in this work, the value of spontaneous magnetization increased with increasing Co content. This result indicates that the interchain spin canceling should also be taken in account. The critical temperature (T_c) shifted toward lower temperature as x increases (Figure 3c and Table S8). From the results of the Curie–Weiss fitting, the effective magnetic moment (μ_{eff}) and Weiss temperature (θ) were determined. The estimated μ_{eff} values agree well with the expected spin-only ones for the sum of Co^{2+} (S = 3/2) and Ni^{2+} (S = 1) according to the formula Co_xNi_{1-x}-MOF-74 (x = 0.752, 0.458, 0.233) (Table S8). As x

decreases, the Weiss temperature (θ) increases from negative (for Co-MOF-74) to positive (for Ni-MOF-74). This tendency clearly indicates a gradual change in the intrachain coupling by substituting Ni for Co. Figure S12a shows magnetization curves of Co-MOF-74, Ni-MOF-74, and Co_xNi_{1-x}-MOF-74 at 2 K. Co_xNi_{1-x}-MOF-74 exhibited hysteresis loops, while Ni-MOF-74 and Co-MOF-74 showed no hysteresis. These phenomena also support Co_xNi_{1-x}-MOF-74 showing canted antiferromagnetism. The coercive field of Co_xNi_{1-x}-MOF-74 was 1490, 1310, 470 Oe, and remnant magnetization was 0.0250, 0.0202, and 0.0066 μ_B, for $x = 0.767$, 0.542, and 0.233, respectively. All magnetization curves exhibited a sigmoidal shape, which is typical of metamagnetic behavior. The values of the critical field (H_c) of metamagnetic transition, which can be calculated as the maximum field of dM/dH, were estimated to be 24000 Oe (Co-MOF-74), 25000 Oe ($Co_{0.8}Ni_{0.2}$-MOF-74), 32500 Oe ($Co_{0.5}Ni_{0.5}$-MOF-74), 35000 Oe ($Co_{0.2}Ni_{0.8}$-MOF-74), and 44000 Oe (Ni-MOF-74), respectively (Table S8). These results indicate that magnetic anisotropy is increased by decreasing x (Co ratio), implying the increase of the interchain coupling. As shown in Figure S12b, the magnetization curves of all the samples showed no hysteresis at 20 K, above the T_c.

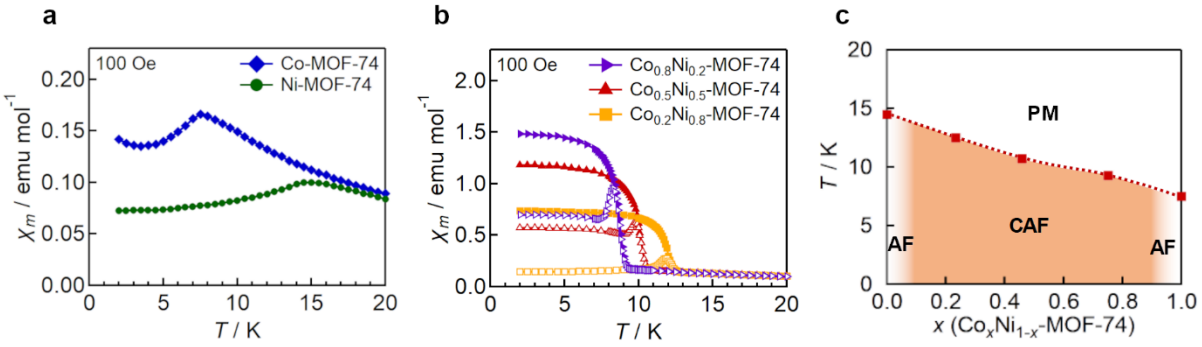

Figure 3. The magnetic susceptibility as a function of temperature for (a) Co-MOF-74 and Ni-MOF-74 and (b) Co_xNi_{1-x}-MOF-74. The open and solid symbols represent zero-field cooled (ZFC)

and field cooled (FC), respectively. (c) Temperature–Co content (T–x) phase diagram of Co_xNi_{1-x}-MOF-74. (PM, paramagnetic phase; AF, antiferromagnetic phase; CAF, canted antiferromagnetic phase.)

We further investigated the effect of the guest adsorption on the magnetic properties for $Co_{0.5}Ni_{0.5}$-MOF-74. We used C_2H_4 as a guest molecule because it is known to bind strongly with open metal sites, which can significantly change the magnetic properties.[18] Figure 4a shows the temperature dependence of magnetic susceptibility of $Co_{0.5}Ni_{0.5}$-MOF-74, as-synthesized and C_2H_4 loaded. Upon C_2H_4 adsorption, the T_c decreased slightly, from 10.7 K (as-synthesized, H_2O adsorbed) to 10.0 K (C_2H_4 adsorbed). From the calculation of $d\chi/dT$, the temperature at which the maximum change occurs decreased from 10.1 K to 7.6 K. To estimate the value of the magnetic interaction, we used the extended Fisher model with an interchain magnetic interaction in the molecular field approximation(Figure S13).[18] The calculated values of intra- and interchain interactions were as follows: $J_{NN} = 3.68$ cm^{-1}, $J_{IC} = -0.88$ cm^{-1} for as-synthesized $Co_{0.5}Ni_{0.5}$-MOF-74, and $J_{NN} = 2.28$ cm^{-1}, $J_{IC} = -0.75$ cm^{-1} for C_2H_4 loaded $Co_{0.5}Ni_{0.5}$-MOF-74 (Table S9). These values suggest that the interchain interaction of $Co_{0.5}Ni_{0.5}$-MOF-74 is weakened by adsorbing C_2H_4, resulting in the decrease of T_c. The magnetization curves also support this speculation (Figure 4b). The value of the critical field (H_c) was slightly shifted from a higher field (32500 Oe) to a lower field (30000 Oe) by adsorbing C_2H_4, indicating a decrease in interchain coupling. Co-MOF-74 and Ni-MOF-74 also showed similar behavior; upon C_2H_4 adsorption, the T_c and H_c were slightly decreased (Figures S14 and S15).

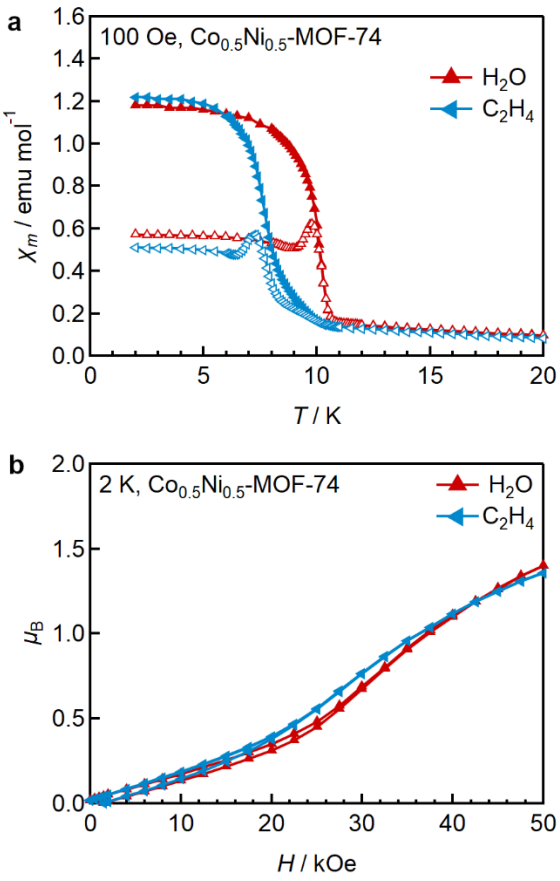

Figure 4. (a) Magnetic susceptibility as a function of temperature for as-synthesized (hydrated) and C_2H_4 adsorbed $Co_{0.5}Ni_{0.5}$-MOF-74. The open and solid symbols represent zero-field cooled (ZFC) and field cooled (FC), respectively. (b) Magnetization curves of as-synthesized (hydrated) and C_2H_4 adsorbed $Co_{0.5}Ni_{0.5}$-MOF-74.

To investigate the structural changes of Co_xNi_{1-x}-MOF-74 by adsorbing C_2H_4 and the effects on magnetism, we measured PXRD patterns for C_2H_4 adsorbed $Co_{0.5}Ni_{0.5}$-MOF-74 at room temperature. The patterns were almost the same as patterns for hydrated (as-synthesized) $Co_{0.5}Ni_{0.5}$-MOF-74, except for a slight peak shift to the higher angle side (Figure S18). We calculated the lattice constants by Rietveld refinement, using the reported structure of C_2H_4

adsorbed Fe-MOF-74[18] as an initial structural model. Compared to the as-synthesized samples, the lattice constant *a* of C_2H_4 adsorbed $Co_{0.5}Ni_{0.5}$-MOF-74 increased and *c* decreased, resulting in a decrease in the distance between the chains (Table S13 and Figure S19). Ni-MOF-74 and Co-MOF-74 also showed a decrease in the interchain distance by adsorbing C_2H_4 (Figure S19). From these results, it is assumed that the cause of the weakened interchain interaction is not the distance between the chains. One possibility is that the change in guest molecule from H_2O to C_2H_4 weakens the interchain interaction via the guest molecule.[26]

CONCLUSION

In summary, we have systematically synthesized a series of mixed-metal Co_xNi_{1-x}-MOF-74 with x = 0.233, 0.542, 0.767 and investigated their magnetic properties. From PXRD, SEM-EDX, and N_2 adsorption measurements, we confirmed the synthesis of isostructural Co_xNi_{1-x}-MOF-74 with homogeneous metal distribution over the whole composition range. Co_xNi_{1-x}-MOF-74 exhibited weak ferromagnetic behavior, while homometallic Co-MOF-74 and Ni-MOF-74 showed antiferromagnetism. The values of spontaneous magnetization were controlled by changing the metal ratio. In addition, we also confirmed that C_2H_4 adsorbed $Co_{0.5}Ni_{0.5}$-MOF-74 exhibited a change in interchain magnetic interaction, accompanied by a shift in H_c and T_c. We envisage that our findings will be useful in the development of applications involving magnetic devices.

ASSOCIATED CONTENT

Supporting Information.

The Supporting Information is available free of charge. Details of the experimental methods, XRF measurement results, Rietveld refinement results, SEM-EDX mappings, nitrogen sorption isotherms, magnetic properties, and DFT calculations (PDF).

AUTHOR INFORMATION

Corresponding Author

Megumi Mukoyoshi − Division of Chemistry, Graduate School of Science, Kyoto University, Sakyo-ku, Kyoto 606-8502, Japan;

Email: mukoyoshi@ssc.kuchem.kyoto-u.ac.jp

Mitsuhiko Maesato − Division of Chemistry, Graduate School of Science, Kyoto University, Sakyo-ku, Kyoto 606-8502, Japan

Email: maesato@ kuchem.kyoto-u.ac.jp

Hiroshi Kitagawa − Division of Chemistry, Graduate School of Science, Kyoto University, Sakyo-ku, Kyoto 606-8502, Japan;

Email: kitagawa@kuchem.kyoto-u.ac.jp

Authors

Shogo Kawaguchi − Research & Utilization Division, Japan Synchrotron Radiation Research Institute (JASRI), SPring-8, Hyogo 679-5198, Japan

Yoshiki Kubota − Department of Physics, Graduate School of Science, Osaka Metropolitan University, Sakai, Osaka 599-8531, Japan

Keigo Cho − Division of Chemical Engineering, Department of Materials Engineering Science, Graduate School of Engineering Science, Osaka University, Toyonaka, Osaka 560-8531, Japan

Yasutaka Kitagawa − Division of Chemical Engineering, Department of Materials Engineering Science, Graduate School of Engineering Science, Osaka University, Toyonaka, Osaka 560-8531, Japan

Author Contributions

All authors have given approval to the final version of the manuscript.

Notes

The authors declare no competing financial interest.

ACKNOWLEDGMENTS

This work was supported by Grant-in-Aid for Specially Promoted Research (20H05623). Synchrotron XRD measurements were performed at SPring-8, supported by the Japan Synchrotron Radiation Research Institute (Proposals 2021A1202).

REFERENCES

(1) Kitagawa, S.; Kitaura, R.; Noro, S.-I. Functional Porous Coordination Polymers. *Angew. Chem. Int. Ed.* **2004**, *43* (18), 2334–2375.

(2) Furukawa, H.; Cordova, K. E.; O'Keeffe, M.; Yaghi, O. M. The Chemistry and Applications of Metal–Organic Frameworks. *Science* **2013**, *341* (6149), 1230444.

(3) Kurmoo, M. Magnetic Metal–Organic Frameworks. *Chem. Soc. Rev.* **2009**, *38* (5), 1353–1379.

(4) Abednatanzi, S.; Derakhshandeh, P. G.; Depauw, H.; Coudert, F.-X.; Vrielinck, H.; Van Der Voort, P.; Leus, K. Mixed-Metal Metal–Organic Frameworks. *Chem. Soc. Rev.* **2019**, *48* (9), 2535–2565.

(5) Masoomi, M. Y.; Morsali, A.; Dhakshinamoorthy, A.; Garcia, H. Mixed-Metal MOFs: Unique Opportunities in Metal‐Organic Framework (MOF) Functionality and Design. *Angew. Chem.* **2019**, *131* (43), 15330–15347.

(6) Fu, Y.; Xu, L.; Shen, H.; Yang, H.; Zhang, F.; Zhu, W.; Fan, M. Tunable Catalytic Properties of Multi-Metal–Organic Frameworks for Aerobic Styrene Oxidation. *Chem. Eng. J.* **2016**, *299*, 135–141.

(7) Dincă, M.; Long, J. R. High-Enthalpy Hydrogen Adsorption in Cation-Exchanged Variants of the Microporous Metal–Organic Framework $Mn_3[(Mn_4Cl)_3(BTT)_8(CH_3OH)_{10}]_2$. *J. Am. Chem. Soc.* **2007**, *129* (36), 11172–11176.

(8) Gao, J.; Qian, X.; Lin, R.-B.; Krishna, R.; Wu, H.; Zhou, W.; Chen, B. Mixed Metal-Organic Framework with Multiple Binding Sites for Efficient C_2H_2/CO_2 Separation. *Angew. Chem. Int. Ed.* **2020**, *59* (11), 4396–4400.

(9) White, K. A.; Chengelis, D. A.; Gogick, K. A.; Stehman, J.; Rosi, N. L.; Petoud, S. Near-Infrared Luminescent Lanthanide MOF Barcodes. *J. Am. Chem. Soc.* **2009**, *131* (50), 18069–18071.

(10) Ferrando-Soria, J.; Serra-Crespo, P.; de Lange, M.; Gascon, J.; Kapteijn, F.; Julve, M.; Cano, J.; Lloret, F.; Pasán, J.; Ruiz-Pérez, C.; Journaux, Y.; Pardo, E. Selective Gas and Vapor Sorption and Magnetic Sensing by an Isoreticular Mixed-Metal–Organic Framework. *J. Am. Chem. Soc.* **2012**, *134* (37), 15301–15304.

(11) Howe, J. D.; Morelock, C. R.; Jiao, Y.; Chapman, K. W.; Walton, K. S.; Sholl, D. S. Understanding Structure, Metal Distribution, and Water Adsorption in Mixed-Metal MOF-74. *J. Phys. Chem. C* **2017**, *121* (1), 627–635.

(12) Wang, Y.-Q.; Yue, Q.; Qi, Y.; Wang, K.; Sun, Q.; Gao, E.-Q. Manganese(II), Iron(II), and Mixed-Metal Metal-Organic Frameworks Based on Chains with Mixed Carboxylate and Azide Bridges: Magnetic Coupling and Slow Relaxation. Inorg. Chem. **2013,** 52 (8), 4259–4268.

(13) Zeng, M. H.; Wang, B.; Wang, X. Y.; Zhang, W. X.; Chen, X. M.; Gao, S. Chiral Magnetic Metal-Organic Frameworks of Dimetal Subunits: Magnetism Tuning by Mixed-Metal Compositions of the Solid Solutions. Inorg. Chem. **2006,** 45 (18), 7069–7076.

(14) Dietzel, P. D. C.; Panella, B.; Hirscher, M.; Blom, R.; Fjellvåg, H. Hydrogen Adsorption in a Nickel Based Coordination Polymer with Open Metal Sites in the Cylindrical Cavities of the Desolvated Framework. *Chem. Commun.* **2006**, *1* (9), 959–961.

(15) Dietzel, P. D. C.; Morita, Y.; Blom, R.; Fjellvåg, H. An In Situ High-Temperature Single-Crystal Investigation of a Dehydrated Metal–Organic Framework Compound and Field-Induced

Magnetization of One-Dimensional Metal–Oxygen Chains. *Angew. Chem. Int. Ed.* **2005**, *44* (39), 6354–6358.

(16) Cadot, S.; Veyre, L.; Luneau, D.; Farrusseng, D.; Alessandra Quadrelli, E. A Water-Based and High Space-Time Yield Synthetic Route to MOF Ni_2(Dhtp) and Its Linker 2,5-Dihydroxyterephthalic Acid. *J. Mater. Chem. A* **2014**, *2* (42), 17757–17763.

(17) Son, K.; Kim, R. K.; Kim, S.; Schütz, G.; Choi, K. M.; Oh, H. Metal Organic Frameworks as Tunable Linear Magnets. *Phys. Status Solidi A* **2020**, *217* (12), 1901000.

(18) Bloch, E. D.; Queen, W. L.; Krishna, R.; Zadrozny, J. M.; Brown, C. M.; Long, J. R. Hydrocarbon Separations in a Metal-Organic Framework with Open Iron(II) Coordination Sites. *Science* **2012**, *335* (6076), 1606–1610.

(19) Caskey, S. R.; Wong-Foy, A. G.; Matzger, A. J. Dramatic Tuning of Carbon Dioxide Uptake via Metal Substitution in a Coordination Polymer with Cylindrical Pores. *J. Am. Chem. Soc.* **2008**, *130* (33), 10870–10871.

(20) Sun, D.; Ye, L.; Sun, F.; García, H.; Li, Z. From Mixed-Metal MOFs to Carbon-Coated Core-Shell Metal Alloy@Metal Oxide Solid Solutions: Transformation of Co/Ni-MOF-74 to CoxNi1-X@CoyNi1-YO@C for the Oxygen Evolution Reaction. *Inorg. Chem.* **2017**, *56* (9), 5203–5209.

(21) Mukoyoshi, M.; Kobayashi, H.; Kusada, K.; Otsubo, K.; Maesato, M.; Kubota, Y.; Yamamoto, T.; Matsumura, S.; Kitagawa, H. Ni@ Onion-like Carbon and Co@ Amorphous Carbon: Control of Carbon Structures by Metal Ion Species in MOFs. *Chem. Commun.* **2021**, *57* (48), 5897–5900.

(22) Nagao, H.; Nishino, M.; Shigeta, Y.; Soda, T.; Kitagawa, Y.; Onishi, T.; Yoshioka, Y.; Yamaguchi, K. Theoretical Studies on Effective Spin Interactions, Spin Alignments and Macroscopic Spin Tunneling in Polynuclear Manganese and Related Complexes and Their Mesoscopic Clusters. *Coord. Chem. Rev.* **2000**, *198* (1), 265–295.

(23) Dzyaloshinsky, I. A Thermodynamic Theory of "Weak" Ferromagnetism of Antiferromagnetics. *J. Phys. Chem. Solids* **1958**, *4* (4), 241–255.

(24) Moriya, T. Anisotropic Superexchange Interaction and Weak Ferromagnetism. *Phys. Rev.* **1960**, *120* (1), 91–98.

(25) Rubio-Giménez, V.; Waerenborgh, J. C.; Clemente-Juan, J. M.; Martí-Gastaldo, C. Spontaneous Magnetization in Heterometallic NiFe-MOF-74 Microporous Magnets by Controlled Iron Doping. *Chem. Mater.* **2017**, *29* (15), 6181–6185.

(26) Zeng, M. H.; Yin, Z.; Tan, Y. X.; Zhang, W. X.; He, Y. P.; Kurmoo, M. Nanoporous Cobalt(II) MOF Exhibiting Four Magnetic Ground States and Changes in Gas Sorption upon Post-Synthetic Modification. *J. Am. Chem. Soc.* **2014**, *136* (12), 4680–4688.

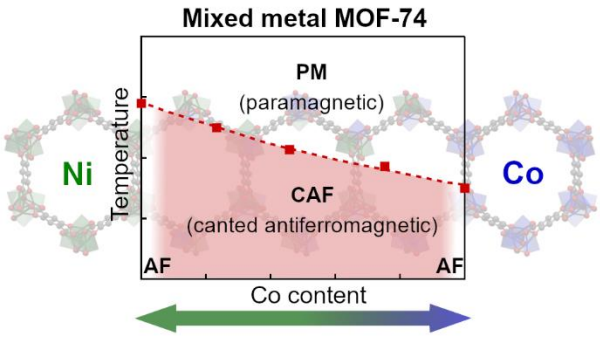

We have systematically investigated the magnetic properties of Co_xNi_{1-x}-MOF-74 ($Co_{2x}Ni_{2(1-x)}$(dhtp), H_4dhtp = 2,5-dihydroxyterephthalic acid) across the composition ranges ($0 \leq x \leq 1$). Bimetallic Co_xNi_{1-x}-MOF-74 ($x = 0.752, 0.458, 0.233$) were successfully synthesized and exhibited weak ferromagnetic (canted antiferromagnetic) behavior, while homometallic Co-MOF-74 and Ni-MOF-74 were antiferromagnetic. We also investigated the effects of C_2H_4 sorption on magnetic properties and found that C_2H_4 adsorbed $Co_{0.5}Ni_{0.5}$-MOF-74 exhibited a change in interchain magnetic interaction.